Taylor & Francis
Taylor & Francis Group

Automatika

Journal for Control, Measurement, Electronics, Computing and Communications

ISSN: 0005-1144 (Print) 1848-3380 (Online) Journal homepage: https://www.tandfonline.com/loi/taut20

Constructing multiwing attractors from a robust chaotic system with non-hyperbolic equilibrium points

Chunlai Li & Wenhua Hai

To cite this article: Chunlai Li & Wenhua Hai (2018) Constructing multiwing attractors from a robust chaotic system with non-hyperbolic equilibrium points, Automatika, 59:2, 184-193, DOI: 10.1080/00051144.2018.1516273

To link to this article: https://doi.org/10.1080/00051144.2018.1516273

Published online: 13 Sep 2018.

AUTOMATIKA
2018, VOL. 59, NO. 2, 184–193
https://doi.org/10.1080/00051144.2018.1516273

REGULAR PAPER

OPEN ACCESS Check for updates

Constructing multiwing attractors from a robust chaotic system with non-hyperbolic equilibrium points

Chunlai Li[a,b] and Wenhua Hai[a]

[a]Department of Physics and Key Laboratory of Low-dimensional Quantum Structures and Quantum Control of Ministry of Education, and Synergetic Innovation Center for Quantum Effects and Applications, Hunan Normal University, Changsha, People's Republic of China; [b]College of Physics and Electronics, Hunan Institute of Science and Technology, Yueyang, People's Republic of China

ABSTRACT

We investigate a three-dimensional (3D) robust chaotic system which only holds two non-hyperbolic equilibrium points, and finds the complex dynamical behaviour of position modulation beyond amplitude modulation. To extend the application of this chaotic system, we initiate a novel methodology to construct multiwing chaotic attractors by modifying the position and amplitude parameters. Moreover, the signal amplitude, range and distance of the generated multiwings can be easily adjusted by using the control parameters, which enable us to enhance the potential application in chaotic cryptography and secure communication. The effectiveness of the theoretical analyses is confirmed by numerical simulations. Particularly, the multiwing attractor is physically realized by using DSP (digital signal processor) chip.

ARTICLE HISTORY
Received 1 February 2018
Accepted 22 August 2018

KEYWORDS
Multiwing attractor; complex dynamical behaviour; digital signal processor

1. Introduction

As an active topic, chaos has been extensively and continuously investigated in classical [1–7] and quantum fields [8,9] over the last half-century. The study on chaos has well served to promote the exploration of dynamical behaviour, intrinsic structure of the natural system and the design of the new chaotic system, as well as chaos-based application. One of the potential applications of chaos is the image encryption and secure communication based on synchronization technology [10–15], since the complicated signal of the chaotic system could be used as a carrier wave or a secure key. It is confirmed that multiwing (or multiscroll) chaotic system can present more complex dynamics than that with few wings (or scrolls) [16].

Since the famous Chua double-scroll circuit was formulated and analysed [17,18], numerous efforts have been exerted to construct and realize multiwing (or multiscroll) chaotic attractors. The basic idea for most of the nonlinear systems to generate multiwing (or multiscroll) attractors is to increase the number of index-2 equilibrium points by introducing multi-segment quadratic function [19,20], polynomial function [21], saw-tooth function [22,23], sinusoidal function [24,25], hysteresis function [26,27], stair function [28–30], transformation function [31], triangle function [21,32] and others. In addition, there exist many other methods to generate multiwing (or multiscroll) chaotic attractors. For example, Yu reported a class of grid multiscroll chaotic attractors by designing switching linear systems and constructing heteroclinic loops [33,34]. Chen introduced a simple method for constructing multiscroll chaotic systems by selecting a proper unstable linear system and implementing shift transformations [35]. Li and Yu proposed a ring-scroll Chua system by introducing a generalized ring transformation [36]. Yu also proposed a general ring-multiscroll system family by introducing a parameterized nth-order polynomial transformation in generalized Lorenz systems [37]. Deng and Lü introduced a switching control scheme for constructing multidirectional multiscroll chaotic attractors in the fractional differential system, which can generate more scroll number than classical model [38]. Tahir presented a class of multiwing attractors with no-equilibrium and with an infinite number of equilibrium points respectively, by using a state feedback controller [39]. Jafari [40], Hu [41], Wang [42] and Escalante-González [43,44] also reported a class of multiscroll system without equilibrium. Bouallegue proposed a family of chaotic attractors with separated multiscrolls by combining the Julia fractal process with Chua's attractor and Lorenz's attractor [45]. Although various design methods emerged, it's still an attractive research interest in seeking new methods for constructing multiwing (or multiscroll) chaotic attractors.

The conception of robust chaos was first introduced by Banerjee when studying the current mode controlled

CONTACT Wenhua Hai whhai2005@aliyun.com Department of Physics and Key Laboratory of Low-dimensional Quantum Structures and Quantum Control of Ministry of Education, and Synergetic Innovation Center for Quantum Effects and Applications, Hunan Normal University, Changsha 410081, People's Republic of China

boost converter [46], which is defined by the absence of periodic windows over some range of the parameter space and chaos is the unique state in this range. Banerjee also found the robust chaos in buck converter and proposed the conditions of robust chaos [47]. Subsequently, based on Banerjee's theorem, Min introduced a chaos robustness criterion for a kind of two-dimensional piecewise smooth map (2DPSM) and constructed a 2DPSM with robust chaos feature [48]. Andrecut confirmed robust chaos in a family of one-dimensional continuous piecewise smooth maps based on bifurcation structure [49]. These investigations only concern the robust chaos feature over a limited parameter range. Recently, we found that there exists robust chaos in the continuous chaotic system over infinite parameter range, and these parameters can regularly control the signal amplitude (which is called amplitude modulation for the convenience), yet the Lyapunov exponents keep invariable [50–54]. Therefore, it is a promising type of system in the practical application of image encryption, signal processing, synchronization and chaotic communication [53,54]. However, as far as we know, little research on such a system, particularly its extension of application, has been done in the present literatures.

This paper aims at developing a systematic methodology for generating multiwing attractors by constructing a robust chaotic system and modifying the position and amplitude parameters of the system. We first introduce a robust chaotic system and analyse the dynamical properties carefully. It's found that the reported system holds two non-hyperbolic equilibrium points and possesses the feature of position modulation (interpreted as controlling the position of the chaotic signal by system parameter), other than amplitude modulation. Then, with the application of position modulation, we realize the double scheme for wing number in the robust chaotic system by modifying the position parameter. And with the application of amplitude modulation, we further construct multiwing chaotic attractors from the modified system by transforming the amplitude parameter. The proposed design philosophy is different from the existing approach in literatures [19–45], and the designing process is concise with only three simple operations. What's more, the signal amplitude, range and distance of the generated wings can be modulated by the control parameters. The reported dynamical behaviours of the multiwing chaotic system are discussed theoretically and confirmed numerically, which displays the potential application in chaotic cryptography and secure communication for the flexible choice of attractor characteristics.

The rest of this paper is outlined as below: in Section2, we introduce a robust chaotic system and discuss the dynamical properties. In Section 3, we give the design scheme and analysis for generating multiwing attractors from the robust chaotic system. In Section 4, we give a DSP-based realization of the multiwing attractor. Finally, the conclusion is drawn in Section 5.

2. Model of robust chaotic system

2.1. Model description

The considered 3D system is described by

$$\begin{cases} \dot{x}_1 = x_2 - a x_1 \\ \dot{x}_2 = -b x_1 - c x_1 x_3 \\ \dot{x}_3 = -h + k {x_2}^2 \end{cases} \tag{1}$$

where $x(t) = (x_1(t), x_2(t), x_3(t))$ are the state variables. The volume contraction of system (1) can be reckoned by the Lie derivative $\nabla V = \partial\dot{x}/\partial x + \partial\dot{y}/\partial y + \partial\dot{z}/\partial z = -a$, which means that system (1) holds a negative dissipativity when $a > 0$. Thereby, system (1) is bounded, and the asymptotic motion at time through the flow will settle onto an attractor.

For the positive parameters a, b, c, h, k, we obtain two equilibrium points of system (1), as below

$$E_+ \left(\frac{1}{a}\sqrt{\frac{h}{k}}, \sqrt{\frac{h}{k}}, -\frac{b}{c} \right), \quad E_- \left(-\frac{1}{a}\sqrt{\frac{h}{k}}, -\sqrt{\frac{h}{k}}, -\frac{b}{c} \right).$$

Then the corresponding characteristic equation at any equilibrium point (x_{E1}, x_{E2}, x_{E3}) is deduced to

$$|J - \lambda I| = -\lambda^3 - a\lambda^2 - (b + c x_{E3} + 2ck x_{E1} x_{E2})\lambda - 2ack x_{E1} x_{E2} \tag{2}$$

When considering the representation of E_+ or E_-, the characteristic equation (2) is simplified as

$$|J - \lambda I| = -\lambda^3 - a\lambda^2 - 2\frac{ch}{a}\lambda - 2ch \tag{3}$$

Equation (3) holds one negative real root $\lambda_1 = -a$ and two pure imaginary roots $\lambda_{2,3} = \pm i\sqrt{2ch/a}$. Therefore, the two equilibrium points are non-hyperbolic, and system (1) doesn't belong to Šil'nikov type chaos.

By selecting the parameter set $S_0 = \{a = 5, b = 1, c = 1, h = 40, k = 1\}$ and the initial condition $x(0) = (0.01, 0.01, 0.05)$, we calculate the three Lyapunov exponents of system (1) as (0.508566, 0, −5.498819) by the orthogonal method [55], confirming the chaotic behaviour. The corresponding chaotic attractors are shown in Figure 1. It can be seen that the chaotic trajectories have two wings alternatively swirling around the two non-hyperbolic equilibrium points.

2.2. Dynamics analysis of amplitude and position modulation

Although there are still many chaotic systems of non-hyperbolic type, little attention is paid to the property of robust chaos for this kind of system, see, for

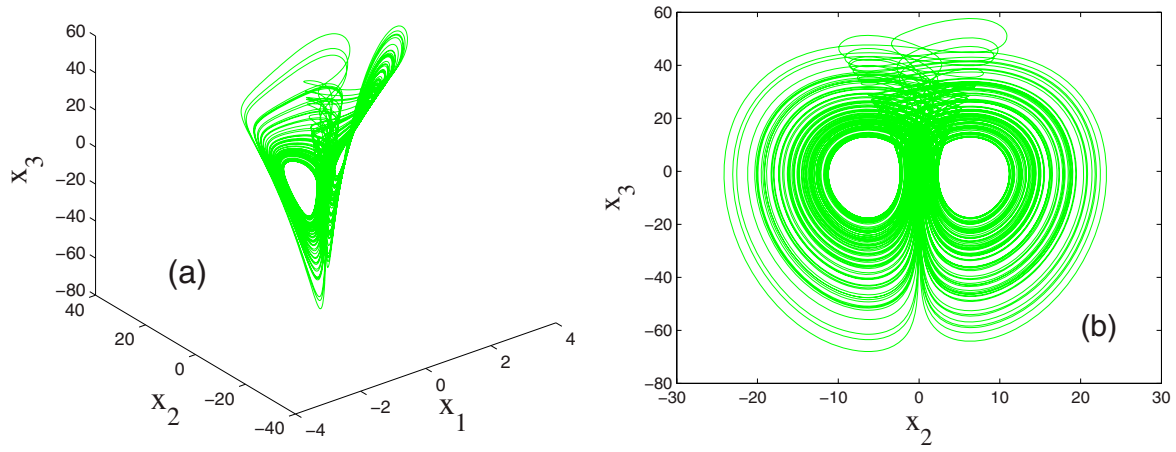

Figure 1. (a) Attractor in the phase space and (b) projection of the attractor onto the plane (x_2, x_3) with the parameter set S_0 and for the initial value $x(0) = (0.01, 0.01, 0.05)$.

instance, Refs [56–58] and Refs therein. Recently, we reported a non-hyperbolic system and investigated the dynamics features of robust chaos and amplitude modulation [59]. Zhu investigated the dynamics features of amplitude and position modulations, but the reported chaotic system is hyperbolic with one saddle and two saddle-foci equilibrium points [60]. In this paper, the dynamics feature of the position modulation in the robust non-hyperbolic system is found for the first time, not confined to the amplitude modulation.

Our analysis starts with the linear transformation $x_1 \to x_1/\sqrt{k}$, $x_2 \to x_2/\sqrt{k}$, $x_3 \to x_3$, based on the relation of the system parameter and the mathematical expression of the nonzero equilibrium point [52]. Thus, system (1) is degenerated to the normalized system about parameter k, as below

$$\begin{cases} \dot{x}_1 = x_2 - a x_1 \\ \dot{x}_2 = -b x_1 - c x_1 x_3 \\ \dot{x}_3 = -h + x_2^2 \end{cases} \tag{4}$$

Therefore, the parameter k can modulate the signal amplitude of variables x_1, x_2 according to $1/\sqrt{k}$, but the amplitude of signal x_3 keeps constant. In addition, we notice that the characteristic equation (3) is irrespective to parameter k, thus the Lyapunov exponent spectrum remains constant when k varies. The feature of amplitude modulation for system (1) is depicted by means of signal amplitude, Lyapunov exponent spectrum and phase diagram for the initial value $x(0) = (0.01, 0.01, 0.05)$, as shown in Figure 2.

Next, when considering the transformation of $x_1 \to x_1, \quad x_2 \to x_2, \quad x_3 \to x_3 + b_k/c$, system (1) is deduced to

$$\begin{cases} \dot{x}_1 = x_2 - a x_1 \\ \dot{x}_2 = -(b + b_k) x_1 - c x_1 x_3 \\ \dot{x}_3 = -h + k x_2^2 \end{cases} \tag{5}$$

Thereby, as the parameter b increases, the position of signal x_3 descends at the speed of $1/c$, while the amplitude and position of signals x_1, x_2 keep invariable. Similarly, we know that characteristic equation (3) is irrespective to the variation of parameter b. Thus, when b changes in a real number field, the Lyapunov exponent spectrum remains invariable. The feature of position modulation for system (1) is illustrated in Figure 3, by means of signal amplitude, Lyapunov exponent spectrum and phase diagram for the initial value $x(0) = (0.01, 0.01, 0.05)$.

It's noticed that for the numerical results depicted by Figures 2 and 3, the Lyapunov exponent spectrums keep fluctuating because of the computational precision and the same initial condition of the system under different parameters k or b. In spite of this, the simulation results agree well with the theoretical analyses.

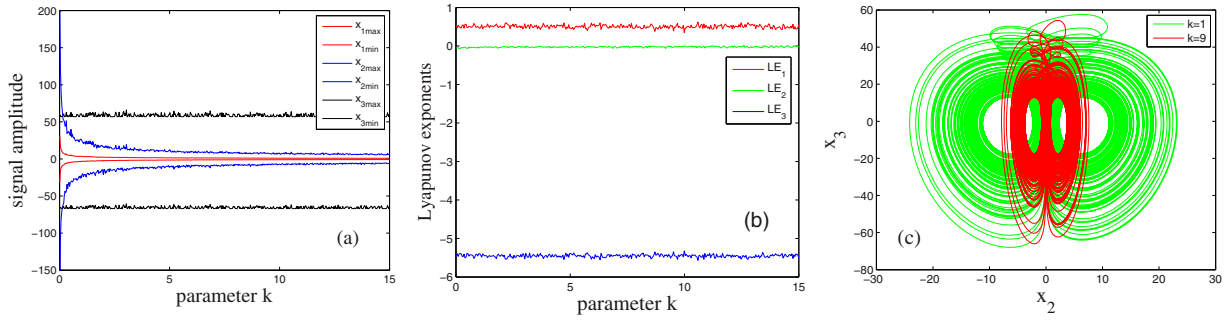

Figure 2. Amplitude modulation interpreted by (a) signal amplitude; (b) Lyapunov exponent spectrum versus parameter k with the parameter set S_0 except for k and (c) phase diagram with different k.

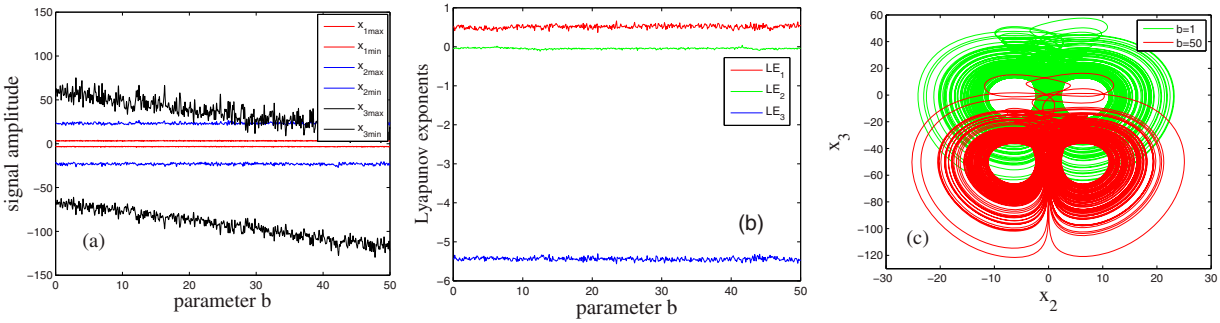

Figure 3. Position modulation interpreted by (a) signal amplitude; (b) Lyapunov exponent spectrum versus parameter b with the parameter set S_0 except for b and (c) phase diagram with different b.

3. Designing multiwing attractors from robust chaotic system

3.1. Design scheme

First of all, we select the parameter set $S_1 = \{a = 5, b = -35, c = 1, h = 40, k = 1\}$ for system (1), then the position of signal x_3 ascends about 36 units, compared with the selection of parameter set S_0, as shown in Figure 4(a). It's known that few trajectories pass through $x_3 = 0$ plane, but most trajectories stay above $x_3 = 0$ plane.

Secondly, to realize the double scheme for wing number in the robust chaotic system, we start with the chaotic system (1) with the parameter set S_1, and make the parameter transformation $b \to b\,sign(x_3)$ by considering the effect of parameter b on signal position. Then the system of differential equations becomes

$$\begin{cases} \dot{x}_1 = x_2 - a x_1 \\ \dot{x}_2 = -b x_1 sign(x_3) - c x_1 x_3 \\ \dot{x}_3 = -h + k x_2^2 \end{cases} \tag{6}$$

where $sign(\cdot)$ is the signum function, which means $sign(x_3) = 1$ for $x_3 > 0$, $sign(x_3) = -1$ for $x_3 < 0$ and $sign(x_3) = 0$ for $x_3 = 0$. When $x_3 > 0$, the equilibrium points for system (6) are $E_1\left(\frac{1}{a}\sqrt{\frac{h}{k}}, \sqrt{\frac{h}{k}}, -\frac{b}{c}\right)$, $E_2\left(-\frac{1}{a}\sqrt{\frac{h}{k}}, -\sqrt{\frac{h}{k}}, -\frac{b}{c}\right)$. And the equilibrium points are $E_3\left(\frac{1}{a}\sqrt{\frac{h}{k}}, \sqrt{\frac{h}{k}}, \frac{b}{c}\right)$, $E_4\left(-\frac{1}{a}\sqrt{\frac{h}{k}}, -\sqrt{\frac{h}{k}}, \frac{b}{c}\right)$ with $x_3 < 0$. The characteristic equation for all these equilibrium points is expressed as (3) through mathematical derivation, therefore, the four equilibrium points are non-hyperbolic. Yet the equilibrium points for $x_3 = 0$ play a key role that bridges the positive half-space and the negative half-space with respect to the x_3-axis. Thus, a four-wing attractor can be generated from system (6), as illustrated in Figure 4(b).

Thirdly, to further construct multiwing chaotic attractors from the modified system (6), we make the parameter transformation $k \to k(1 - k_1 f(k_2 x_2))$ by considering the effect of parameter k on signal amplitude. Then it yields the following resulting system

$$\begin{cases} \dot{x}_1 = x_2 - a x_1 \\ \dot{x}_2 = -b x_1 sign(x_3) - c x_1 x_3 \\ \dot{x}_3 = -h + k(1 - k_1 f(k_2 x_2)) x_2^2 \end{cases} \tag{7}$$

In system (7), $f(\cdot)$ is a periodic function; k_1 and k_2 are the control parameters, which can control the variation ranges of the signal amplitude and the wing distance, respectively. There exist different choices of the function $f(\cdot)$ for the generation of multiwing attractors. For simplicity, we will focus on the case of $f(\cdot) = sin(\cdot)$ in this paper, though similar results and analysis can be made for other periodic functions. Then system (7) can

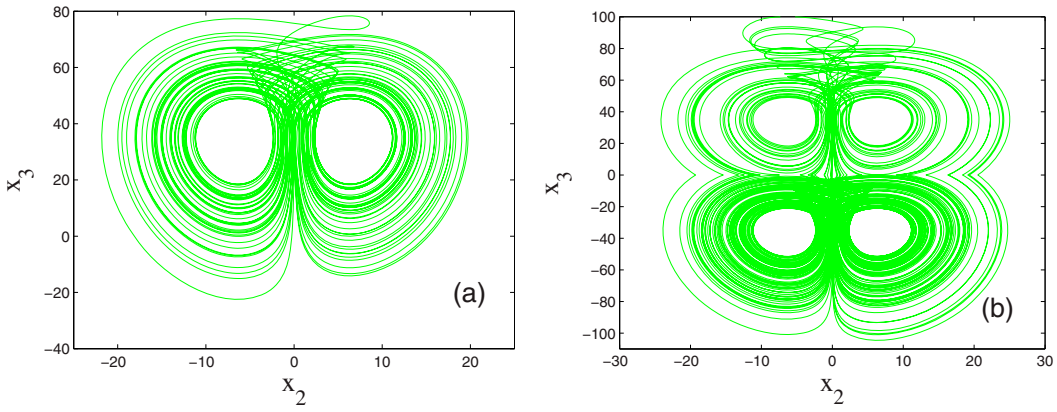

Figure 4. (a). Projection of the attractor for system (1) and (b) projection of the four-wing attractor for system (6) onto the plane (x_2, x_3), with the parameter set S_1 and for the initial condition $x(0) = (0.01, 0.01, 0.05)$.

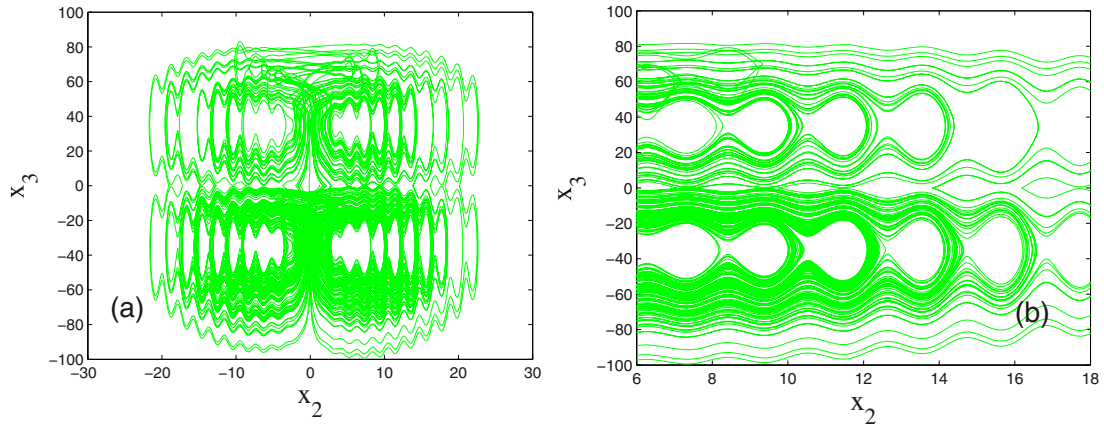

Figure 5. (a) Projection of the attractor for system (8) onto the plane (x_2, x_3) with the parameter set $S_1, k_1 = 3.6, k_2 = 3$ and for the initial condition $x(0) = (0.2, 1.2, 0.5)$ and (b) the enlarged view.

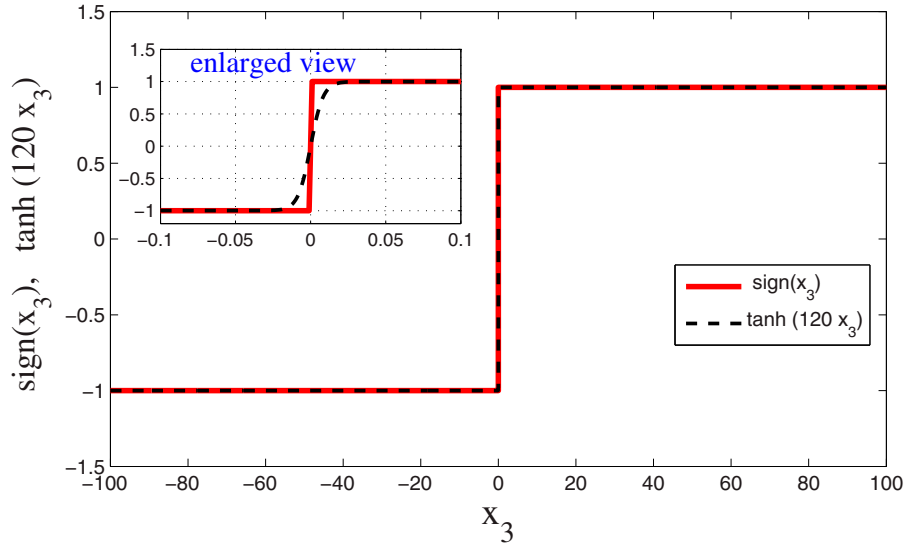

Figure 6. The graph of $sign(x_3)$ and $tanh(120x_3)$.

be reformulated as

$$\begin{cases} \dot{x}_1 = x_2 - ax_1 \\ \dot{x}_2 = -bx_1 sign(x_3) - cx_1x_3 \\ \dot{x}_3 = -h + k(1 - k_1 \sin(k_2x_2))x_2^2 \end{cases} \tag{8}$$

With the selection of the parameter set S_1 and $k_1 = 3.6$, $k_2 = 3$, the numeral simulations of the attractor projected onto the plane (x_2, x_3) in Figure 5 shows that system (8) holds complicated multiwing attractors. The corresponding Lyapunov exponents are reckoned as 0.594554, 0, −5.574220, which further proves the chaotic character. It is worth mentioning that we approximate the signum function $sign(x_3)$ by the hyperbolic function $tanh(120x_3)$, as shown in Figure 6, to reduce differential buffeting when calculating Lyapunov exponents [61].

The diagram of bifurcation and the maximal Lyapunov exponent spectrum is computed by varying parameter c from its null value to detect the dynamical transition. As found in Figure 7, the system reaches a chaotic pattern immediately from the lowest value of c. And we notice that periodic windows embedded in the chaotic region are observed as the value of c is increased.

3.2. Analysis of attractor

In this subsection, we will consider the influences of parameters k, k_1 and k_2 on the characteristics of the generated wing attractors.

The bifurcation diagram for $k \in [0, 10]$ is plotted in Figure 8 to describe the amplitude evolution. Superficially, it seems that the coefficient k can modulate the signal amplitude regularly. But one notices with the careful observation that there emerge visible periodic windows in the chaotic region. In fact, we know that the value of $k(1 - k_1 \sin(k_2x_2))$ changes with parameter k. In this sense, one may guess that if the multiwing attractors exist, k is a parameter that directly affects the signal amplitudes of x_1, x_2 by the power function with the index $-1/2$, but the amplitude of x_3 keeps invariable. The above analysis can be intuitively confirmed by

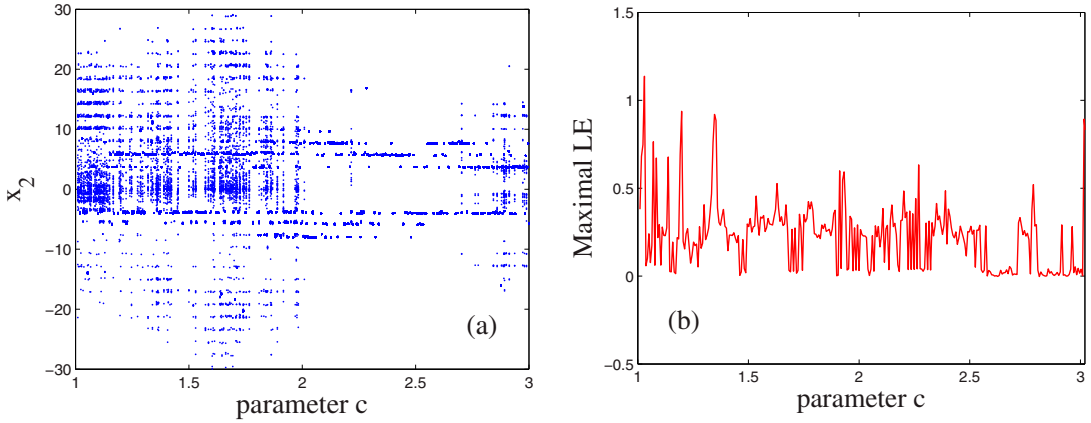

Figure 7. State evolution interpreted by (a) bifurcation diagram and (b) maximal Lyapunov exponent spectrum versus c with the parameter set S_1 except for c, $k_1 = 3.6$, $k_2 = 3$ and for the initial condition $x(0) = (0.2, 0.2, 0.5)$.

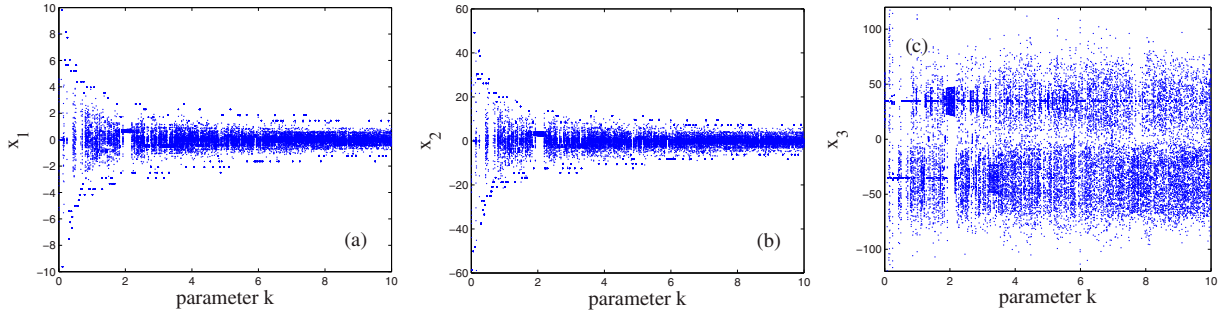

Figure 8. Bifurcation diagrams of (a) x_1, (b) x_2 and (c) x_3 versus k with parameter set S_1 except for k, $k_1 = 3.6$, $k_2 = 3$ and for the initial condition $x(0) = (0.2, 0.2, 0.5)$.

numerical results with $k = 1$ and $k = 4$, as respectively described in Figure 9.

We now analyse the influence of control parameter k_1 on the property of the generated wings. It's obvious that a larger value of k_1 will yield a wider variation range of $k(1 - k_1 \sin(k_2 x_2))$. As a result, if the multiwing chaotic attractors exist, the variation ranges of the signal amplitude of x_1, x_2 increase with a larger k_1. In other words, the range from the innermost wing to the outermost wing in x_1, x_2 direction increase with a larger k_1. The analysis is compared in Figure 10 with $k_1 = 1$ and Figure 11 with $k_1 = 4$ by numerical simulations.

Finally, we consider the role of k_2. It's noticed that $\sin(k_2 x_2)$ is a function with the period as $2\pi/k_2$, which means that the right-hand side of the third equation of system (8) keeps invariable when x_2 moves to $x_2 + 2m\pi/k_2$, $m \in Z$. Therefore, if these multiwing chaotic attractors exist, the distance of adjacent wings (called wing distance for the convenience) can be estimated as $d = 2\pi/k_2$. And we further know that a larger k_2 will bring a smaller distance d. In this sense, parameter k_2

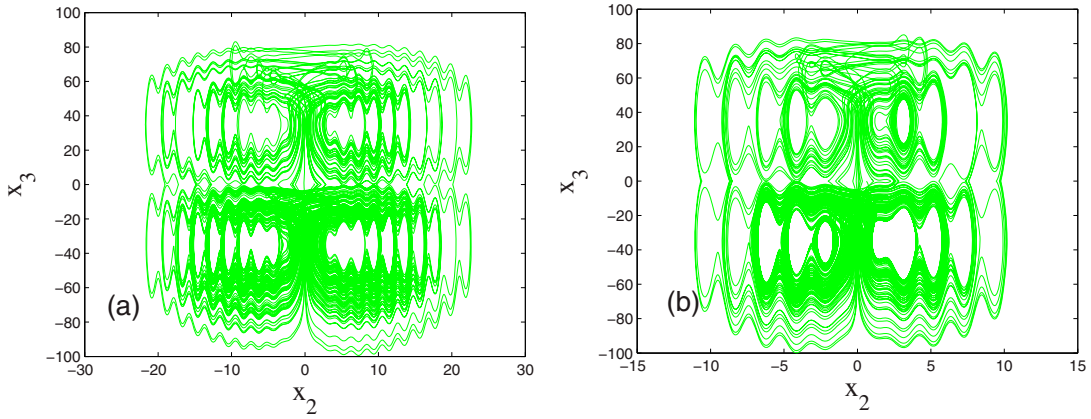

Figure 9. Projection of the attractor for system (8) onto the plane (x_2, x_3) with $a = 5$, $b = -35$, $c = 1$, $h = 40$, $k_1 = 3.6$, $k_2 = 3$ and for (a) $k = 1$, initial condition (0.2, 1.2, 0.5); (b) $k = 4$, initial condition $x(0) = (-0.1, 0.618, -0.1)$.

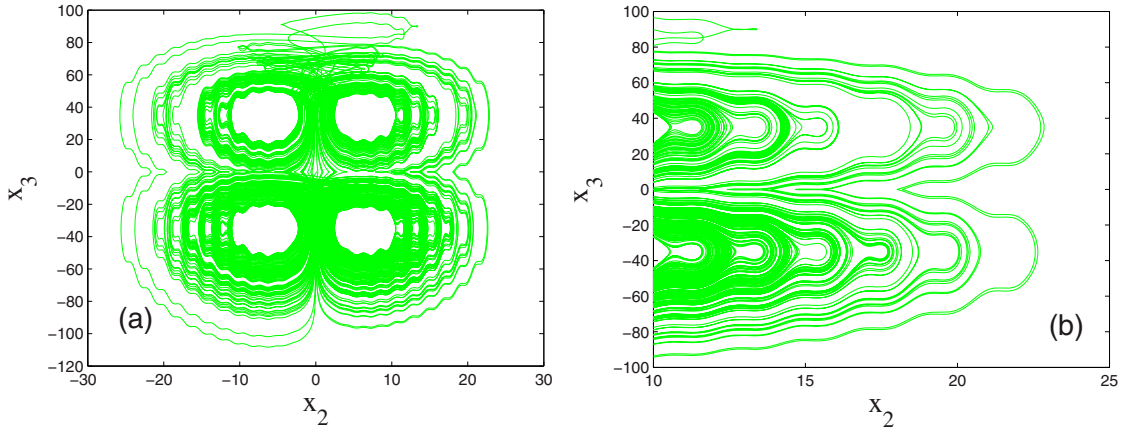

Figure 10. (a) Projection of the attractor for system (8) onto the plane (x_2, x_3) with the parameter set S_1, $k_2 = 3$, $k_1 = 1$ and initial condition $x(0) = (0.2, 0.1, 0.2)$; (b) the enlarged view.

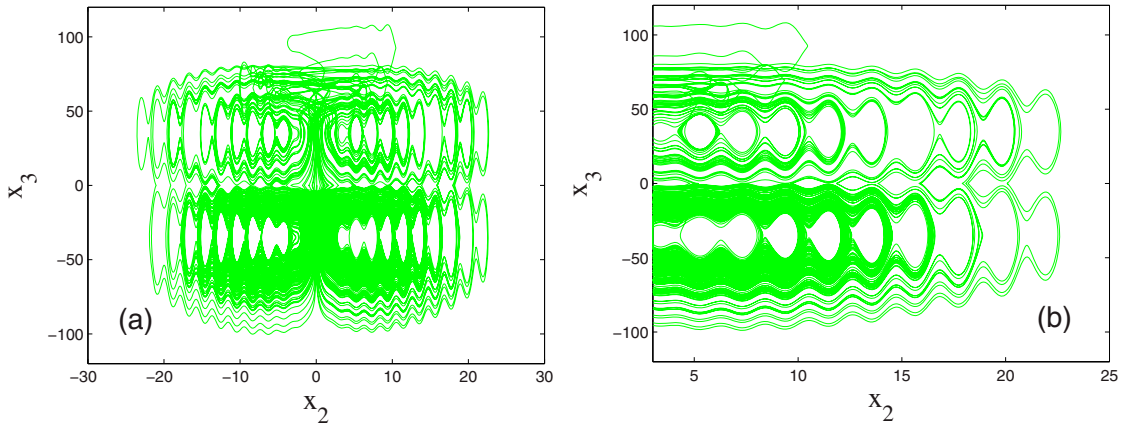

Figure 11. (a) Projection of the attractor for system (8) onto the plane (x_2, x_3) with the parameter set S_1, $k_2 = 3$, $k_1 = 4$ and initial condition $x(0) = (0.02, 0.11, 0.1)$; (b) the enlarged view.

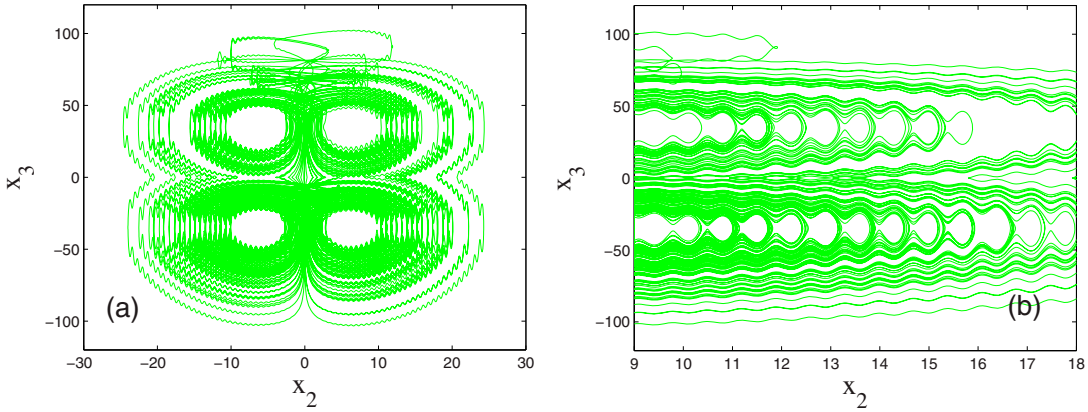

Figure 12. (a) Projection of the attractor for system (8) onto the plane (x_2, x_3) with the parameter set S_1, $k_1 = 3.6$, $k_2 = 9$, and initial condition $x(0) = (0.2, 1.8, -1.2)$; (b) the enlarged view.

can directly affect the wing distance. The analysis can be verified numerically in Figure 5 with $k_2 = 3$ and Figure 12 with $k_2 = 9$.

4. DSP-based realization of the multiwing system

As a microprocessor designed with a special structure, DSP chip holds the features of programmability, flexible interface and high operation speed. Therefore, DSP chip plays an increasingly important role on electronic products research and digital signal processing. In this realization, we adopt TMS320C6747 device, which is a low-power digital signal processor based on a TMS320C674x DSP core with 64-bit running at 375 MHz and floating-point operation, therefore, it is considered to be sufficient for our experiment.

To increase the computational precision of the iterative equation and compress the range of state variables, the variable-scale reduction is first made on system (8). Considering the condition of $a = 5$, $b = -35$, $c = 1$, $h = 40$, $k = 1$, $k_1 = 3.6$, $k_2 = 3$, and the compression

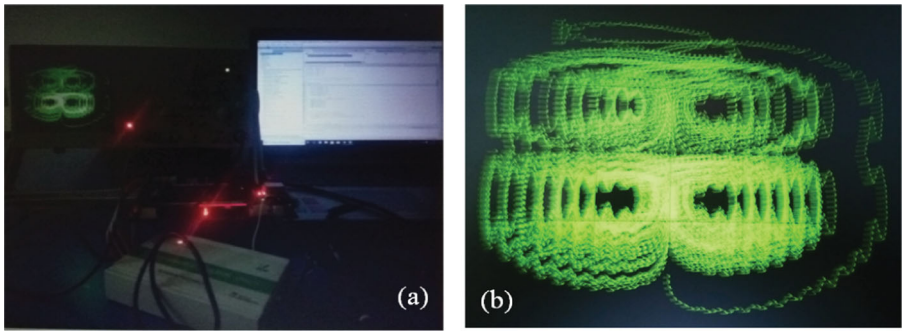

Figure 13. DSP implementation of the multiwing system (a) experimental setup; (b) experimental observation.

factors (2, 6, 25) for variables (x_1, x_2, x_3), we derive the differential equations system of (8) as

$$\begin{cases} \dot{x}_1 = 3x_2 - 5x_1 \\ \dot{x}_2 = \frac{35}{3}x_1 sign(x_3) - \frac{25}{3}x_1x_3 \\ \dot{x}_3 = -\frac{8}{5} + \frac{36}{25}(1 - 3.6\sin(18x_2))x_2{}^2 \end{cases} \tag{9}$$

And we further execute the time-scale transformation to increase the density of periodic orbits and to capture the wave easily. Subsequently, we obtain the resulted system of (9) with the time-scale factor 10, depicted by

$$\begin{cases} \dot{x}_1 = 30x_2 - 50x_1 \\ \dot{x}_2 = \frac{350}{3}x_1 sign(x_3) - \frac{250}{3}x_1x_3 \\ \dot{x}_3 = -16 + 14.4(1 - 3.6\sin(18x_2))x_2^2 \end{cases} \tag{10}$$

Considering that DSP is a digital processor, we discretize the continuous system (10) by the classical Runge–Kutta method with step 0.001. Accordingly, we convert the chaotic digital sequences into analog ones by the multichannel DAC (digital analog converter with the model DAC7724). With the setting of the initial value (0.2, 1.2, 0.5), the oscilloscope observation of the multiwing chaotic attractor is displayed in Figure 13. Compared with the attractors simulated by Matlab in Figure 5, it can be concluded that they have a good qualitative agreement.

5. Conclusion

Robust chaos is an interesting research field of continuing concern and should be paid closer attention to the dynamics and the application expansion. In this paper, we reported a robust chaotic system with amplitude modulation. And for the first time, we found the properties of position modulation and non-hyperbolic equilibrium points swirled around by wings alternatively in the robust chaotic system. By transforming the forms of position parameter and amplitude parameter, a systematic methodology was presented to construct multiwing attractors from the robust chaotic system. The flexible adjustment of the signal amplitude, range and distance of generated wings by changing the control parameters will add the dynamics complexity of the multiwing system, and consequently will enhance the potential application in chaotic cryptography and secure communication. The non-reported design method of multiwing attractors expanded the application range of robust chaos, and will also consequently enrich the design theory of complicated chaotic system.

Disclosure statement

No potential conflict of interest was reported by the authors.

Funding

This work was supported by the NNSF of China [grant number 11475060]; the Research Foundation of Education Bureau of Hunan Province of China [grant number 16B113]; the China Postdoctoral Science Foundation [grant number 2016M590745]; Science and Technology Program of Hunan Province [grant number 2016TP1021]; Hunan Provincial Natural Science Foundation of China [grant number 2016JJ4036].

References

[1] Kim D, Jin M, Chang PH. Control and synchronization of the generalized Lorenz system with mismatched uncertainties using backstepping technique and time-delay estimation. Int J Circ Theor App. 2017;45:1833–1848.
[2] Saberi Nik H, Effati S, Saberi-Nadjafi J. Ultimate bound sets and exponential finite-time synchronization for a complex chaotic system. J Complex. 2015;31:715–730.
[3] Kengne R, Tchitnga R, Mezatio A, et al. Finite-time synchronization of fractional-order simplest two-component chaotic oscillators. Eur Phys J B. 2017;90:88.
[4] La Rosa M, Rabinovich MI, Huerta R, et al. Slow regularization through chaotic oscillation transfer in an unidirectional chain of Hindmarsh-Rose models. Phys Lett A. 2000;266:88–93.
[5] Fortuna L, Arena P, Balya D, et al. Cellular neural networks: a paradigm for nonlinear spatio-temporal processing. IEEE Circ Syst Mag. 2001;1:6–21.
[6] Buscarino A, Fortuna L, Frasca M, et al. Design of time-delay chaotic electronic circuits. IEEE Trans Circuits-I. 2011;58:1888–1896.
[7] Luo R, Zeng Y. The control and synchronization of a rotational relativistic chaotic system with parameter uncertainties and external disturbance. J Comput Nonlin Dyn. 2015;10(6):064503.

[8] Cao H, Wiersig J. Dielectric microcavities: model systems for wave chaos and non-Hermitian physics. Rev Mod Phys. 2015;87:61–111.
[9] Tan J, Zou M, Luo Y, et al. Controlling chaos-assisted directed transport via quantum resonance. Chaos. 2016;26:063106.
[10] Ren HP, Baptista MS, Grebogi C. Wireless communication with chaos. Phys Rev Lett. 2013;110:184101.
[11] Gámez-Guzmán L, Cruz-Hernández C, López-Gutiérrez RM, et al. Synchronization of Chua's circuits with multi-scroll attractors: application to communication. Commun Nonlinear Sci Numer Simul. 2009;14:2765–2775.
[12] Li CC, Liu YS, Zhang LY, et al. Cryptanalyzing a class of image encryption schemes based on Chinese remainder theorem. Signal Process Image. 2014;29:914–920.
[13] Mata-Machuca JL, Martínez-Guerra R, Aguilar-López R, et al. A chaotic system in synchronization and secure communications. Commun Nonlinear Sci Numer Simulat. 2012;17:1706–1713.
[14] Luo YL, Du MH, Liu JX. A symmetrical image encryption scheme in wavelet and time domain. Commun Nonlinear Sci Numer Simul. 2015;20:447–460.
[15] Peng F, Gong X, Long M, et al. A selective encryption scheme for protecting H. 264/AVC video in multimedia social network. Multimed Tools Appl. 2017;76(3):3235–3253.
[16] Trejo-Guerra R, Tlelo-Cuautle E, Cruz-Hernandez C, et al. Chaotic communication system using Chua's oscillators realized with CCII+s. Int J Bifurcat Chaos. 2009;19:4217–4226.
[17] Chua LO, Komuro M, Matsumoto T. The double scroll family. IEEE Trans Circuits Syst-I. 1986;33:1072–1118.
[18] Mees A, Chap man P. Homoclinic and heteroclinic orbits in the double scroll attractor. IEEE Trans Circuits Syst. 1987;34:1115–1120.
[19] Yu S, Tang WKS, Lü J, et al. Generation of n×m-wing Lorenz-like attractors from a modified Shimizu–Morioka model. IEEE Trans Circuits Syst-II. 2008;55:1168–1172.
[20] Yu S, Tang WKS, Lü J, et al. Generating 2n-wing attractors from Lorenz-like systems. Int J Circ Theor App. 2010;38:243–258.
[21] Chen SB, Zeng YC, Xu ML, et al. Construction of grid multi-scroll chaotic attractors and its circuit implementation with polynomial and step function. Acta Phys Sin. 2011;60:020507.
[22] Wang F, Liu C. Generation of multi-scroll chaotic attractors via the saw-tooth function. Int J Mod Phys B. 2008;22:2399–2405.
[23] Trejo-Guerra R, Tlelo-Cuautle E, Jimenez-Fuentes JM, et al. Integrated circuit generating 3-and 5-scroll attractors. Commun Nonlinear Sci Numer Simulat. 2012;17:4328–4335.
[24] Tang WK, Zhong GQ, Chen G, et al. Generation of n-scroll attractors via sine function. IEEE Trans Circuits Syst-I. 2001;48:1369–1372.
[25] Ma J, Wu X, Chu R, et al. Selection of multi-scroll attractors in Jerk circuits and their verification using Pspice. Nonlinear Dyn. 2014;76:1951–1962.
[26] Yu S, Tang WKS. Generation of n× m-scroll attractors in a two-port RCL network with hysteresis circuits. Chaos Soliton Fract. 2009;39:821–830.
[27] Lü J, Han F, Yu X, et al. Generating 3-D multi-scroll chaotic attractors: A hysteresis series switching method. Automatica (Oxf). 2004;40:1677–1687.
[28] Deng WH. Generating 3-D scroll grid attractors of fractional differential systems via stair function. Int J Bifurcat Chaos. 2007;17:3965–3983.
[29] Wang CH, Xu H, Yu F. A novel approach for constructing high-order Chua's circuit with multi-directional multi-scroll chaotic attractors. Int J Bifurcat Chaos. 2013;23:1350022.
[30] Wang Z, Tang H, Chen Z. The design and implementation of a multi-wing chaotic attractor based on a five-term three-dimension system. Int J Circ Theor Appl. 2016;44:1186–1201.
[31] Yu B, Hu GS. Constructing multiwing hyperchaotic attractors. Int J Bifurcat Chaos. 2010;20:1002601.
[32] Chen D, Sun Z, Ma X, et al. Circuit implementation and model of a new multi-scroll chaotic system. Int J Circ Theor Appl. 2014;42:407–424.
[33] Yu S, Lü J, Chen G, et al. Generating grid multiwing chaotic attractors by constructing heteroclinic loops into switching systems. IEEE Trans Circuits Syst-II. 2011;58:314–318.
[34] Yu S, Lü J, Yu X, et al. Design and implementation of grid multiwing hyperchaotic Lorenz system family via switching control and constructing super-heteroclinic loops. IEEE Trans Circuits Syst-I. 2012;59:1015–1028.
[35] Chen L, Peng HJ, Wang DS. Studies on the construction method of a family of multi-scroll chaotic systems. Acta Phys Sin. 2008;57:3337–3341.
[36] Li C, Yu S, Luo X. A ring-scroll Chua system. Int J Bifurcation Chaos. 2013;23:1350170.
[37] Yu S, Lü J, Tang WK, et al. A general multiscroll Lorenz system family and its realization via digital signal processors. Chaos. 2006;16:033126.
[38] Deng W, Lü J. Design of multidirectional multiscroll chaotic attractors based on fractional differential systems via switching control. Chaos. 2006;16:043120.
[39] Tahir FR, Jafari S, Pham VT, et al. A novel no-equilibrium chaotic system with multiwing butterfly attractors. Int J Bifurcat Chaos. 2015;25:1550056.
[40] Jafari S, Pham VT, Kapitaniak T. Multiscroll chaotic sea obtained from a simple 3D system without equilibrium. Int J Bifurcat Chaos. 2016;26:1650031.
[41] Hu X, Liu C, Liu L, et al. Multi-scroll hidden attractors in improved Sprott A system. Nonlinear Dyn. 2016;86:1725–1734.
[42] Zhou L, Wang C, Zhou L. A novel no-equilibrium hyperchaotic multi-wing system via introducing memristor. Int J Circ Theor Appl. 2018;46:84–98.
[43] Escalante-González RJ, Campos-Cantón E, Nicol M. Generation of multi-scroll attractors without equilibria via piecewise linear systems. Chaos. 2017;27:053109.
[44] Escalante-Gonzalez RJ, Campos-Canton E. Generation of chaotic attractors without equilibria via piecewise linear systems. Int J Mod Phys C. 2017;28:1750008.
[45] Bouallegue K. Chaotic attractors with separated scrolls. Chaos. 2015;25:073108.
[46] Banerjee S, Yorke JA, Grebogi C. Robust chaos. Phys Rev Lett. 1998;80:3049–3052.
[47] Banerjee S, Grebogi C. Border collision bifurcations in two-dimensional piecewise smooth maps. Phys Rev E. 1999;59:4052–4061.
[48] Han D, Min L, Hao L. A chaos robustness criterion for 2D piecewise smooth Map with applications in pseudo-random number generator and image encryption with avalanche effect. Math Probl Eng. 2016;2016:1–14.
[49] Andrecut M, Ali MK. Robust chaos in smooth unimodal maps. Phys Rev E. 2001;64:025203.

[50] Zhou XY. A chaotic system with invariable Lyapunov exponent and its circuit simulation. Acta Phys Sin. 2011;60:100503.
[51] Li C, Wu L, Li H, et al. A novel chaotic system and its topological horseshoe. Nonlinear Anal Model Control. 2013;18:66–77.
[52] Jiang J, Wu QQ. A new three-dimensional chaotic system with constant exponent spectrum: analysis, synchronization and circuit implementation. J Softw. 2016;11:494–511.
[53] Li C, Su K, Zhang J. Amplitude control and projective synchronization of a dynamical system with exponential nonlinearity. Appl Math Model. 2015;39:5392–5398.
[54] Li C, Zhang J. Synchronization of a fractional-order chaotic system using finite time input-to-state stability. Int J Syst Sci. 2016;47:2440–2448.
[55] Geist K, Parlitz U, Lauterborn W. Comparison of different methods for computing Lyapunov exponents. Prog Theor Phys. 1990;83:875–893.
[56] Chen B, Han X. Analysis of dynamical behaviors in a continuous chaotic system without Šil'nikov orbits. Int J Bifurcat Chaos. 2015;25:1550014.
[57] Elhadj Z, Sprott JC. On the non-existence of Shilnikov chaos in continuous-time systems. Appl Math Mech. 2012;33:353–356.
[58] Gotthans T, Petržela J. New class of chaotic systems with circular equilibrium. Nonlinear Dyn. 2015;81:1143–1149.
[59] Li C, Xiong J. A simple chaotic system with non-hyperbolic equilibria. Optik (Stuttg). 2017;128:42–49.
[60] Zhu L, Yao KM, Hua ZY, et al. Robust chaotic system with controlled position and exponential term. J Yunnan Normal Univer. 2016;38:232–237.
[61] Yu S, Lü J, Chen G, et al. Design and implementation of grid multiwing butterfly chaotic attractors from a piecewise Lorenz system. IEEE Trans Circuits-II Express Briefs. 2010;57:803–807.